



**Nanosilica Modification of Elastomer-Modified  
VARTM Epoxy Resins for Improved Resin  
and Composite Toughness**

**by Jason Robinette, Andres Bujanda, Daniel DeSchepper, Jessica Dibelka,  
Phillip Costanzo, Robert Jensen, and Steven McKnight**

**ARL-TR-4084**

**April 2007**

## **NOTICES**

### **Disclaimers**

The findings in this report are not to be construed as an official Department of the Army position unless so designated by other authorized documents.

Citation of manufacturer's or trade names does not constitute an official endorsement or approval of the use thereof.

Destroy this report when it is no longer needed. Do not return it to the originator.

# **Army Research Laboratory**

Aberdeen Proving Ground, MD 21005-5069

---

---

**ARL-TR-4084**

**April 2007**

---

## **Nanosilica Modification of Elastomer-Modified VARTM Epoxy Resins for Improved Resin and Composite Toughness**

**Jason Robinette, Andres Bujanda, Daniel DeSchepper, Jessica Dibelka,  
Phillip Costanzo, Robert Jensen, and Steven McKnight  
Weapons and Materials Research Directorate, ARL**

REPORT DOCUMENTATION PAGE			Form Approved OMB No. 0704-0188		
Public reporting burden for this collection of information is estimated to average 1 hour per response, including the time for reviewing instructions, searching existing data sources, gathering and maintaining the data needed, and completing and reviewing the collection information. Send comments regarding this burden estimate or any other aspect of this collection of information, including suggestions for reducing the burden, to Department of Defense, Washington Headquarters Services, Directorate for Information Operations and Reports (0704-0188), 1215 Jefferson Davis Highway, Suite 1204, Arlington, VA 22202-4302. Respondents should be aware that notwithstanding any other provision of law, no person shall be subject to any penalty for failing to comply with a collection of information if it does not display a currently valid OMB control number. <b>PLEASE DO NOT RETURN YOUR FORM TO THE ABOVE ADDRESS.</b>					
1. REPORT DATE (DD-MM-YYYY) April 2007		2. REPORT TYPE Final		3. DATES COVERED (From - To) 5 June 2006–6 February 2007	
4. TITLE AND SUBTITLE Nanosilica Modification of Elastomer-Modified VARTM Epoxy Resins for Improved Resin and Composite Toughness			5a. CONTRACT NUMBER		
			5b. GRANT NUMBER		
			5c. PROGRAM ELEMENT NUMBER		
6. AUTHOR(S) Jason Robinette, Andres Bujanda, Daniel DeSchepper, Jessica Dibelka, Phillip Costanzo, Robert Jensen, and Steven McKnight			5d. PROJECT NUMBER AH84		
			5e. TASK NUMBER		
			5f. WORK UNIT NUMBER		
7. PERFORMING ORGANIZATION NAME(S) AND ADDRESS(ES) U.S. Army Research Laboratory AMSRD-ARL-WM-MA Aberdeen Proving Ground, MD 21005-5069			8. PERFORMING ORGANIZATION REPORT NUMBER ARL-TR-4084		
9. SPONSORING/MONITORING AGENCY NAME(S) AND ADDRESS(ES)			10. SPONSOR/MONITOR'S ACRONYM(S)		
			11. SPONSOR/MONITOR'S REPORT NUMBER(S)		
12. DISTRIBUTION/AVAILABILITY STATEMENT Approved for public release; distribution is unlimited.					
13. SUPPLEMENTARY NOTES					
14. ABSTRACT Recent publications have reported a synergy between rubber and silica in modified epoxy resins that results in significantly improved fracture toughness without reductions in other material properties. In this work, we seek to achieve the same type of synergy in commercial vacuum-assisted resin transfer molding (VARTM) epoxy resins, SC15 and SC79, produced by Applied Polymeric, Inc. Nanopox F400 (Hanse Chemie) containing 40 weight-percent epoxy-functional silica in a diglycidyl bisphenol-F (DGEBF) epoxy was blended with the VARTM resins to add various silica loadings in the systems. It was found that the presence of DGEBF influenced resin properties more than silica. This monomer impacted crosslink density and other material properties. The crosslink density of SC15 was increased and resulted in reductions in resin fracture toughness, mode II composite fracture toughness, and increased damage area in impact performance. The crosslink density of SC79 was reduced upon the addition of DGEBF contained in the Nanopox. At 10 weight-percent silica, resin fracture toughness, mode II composite toughness, and impact properties were improved due to decreased matrix crosslink density and the presence of silica. Finally, morphological studies showed that silica influences the rubber phase separation in a model epoxy system and VARTM epoxies. Further research will investigate the effects of epoxy-functional silica addition to phase separation mechanisms in rubber-toughened epoxies.					
15. SUBJECT TERMS nanosilica, rubber toughening, VARTM, epoxy, mode II, end notch flexure					
16. SECURITY CLASSIFICATION OF:			17. LIMITATION OF ABSTRACT	18. NUMBER OF PAGES	19a. NAME OF RESPONSIBLE PERSON
a. REPORT	b. ABSTRACT	c. THIS PAGE			Jason Robinette
UNCLASSIFIED	UNCLASSIFIED	UNCLASSIFIED	UL	28	19b. TELEPHONE NUMBER (Include area code) 410-306-2100

---

## Contents

---

<b>List of Figures</b>	<b>iv</b>
<b>List of Tables</b>	<b>iv</b>
<b>Acknowledgments</b>	<b>v</b>
<b>1. Introduction</b>	<b>1</b>
<b>2. Experimental</b>	<b>2</b>
2.1 Materials and Resin Formulations.....	2
2.2 Resin Characterization .....	3
2.3 Composite Characterization .....	4
2.4 Morphological Characterization.....	7
<b>3. Results and Discussion</b>	<b>8</b>
3.1 Resin Properties.....	8
3.2 Composite Properties .....	10
3.3 Comparisons Between Model and VARTM Epoxies .....	13
<b>4. Conclusion</b>	<b>16</b>
<b>5. References</b>	<b>17</b>
<b>Distribution List</b>	<b>19</b>

---

## List of Figures

---

Figure 1. Sample geometry of ENF specimens. ....	4
Figure 2. Alternative ESIS crack initiation criteria for ENF test methods (10). ....	5
Figure 3. A plot of fracture toughness ( $G_{1c}$ ) as a function of silica concentration in SC15 and SC79 resins. A rules-of-mixture line is shown for each resin that accounts for the change in fracture toughness as a result of blending DGEGBF into the formulation.....	9
Figure 4. Digital images of the composite strike face after drop tower impact testing. Imaging software is used to calculate the damage area. Each panel image is 100 × 100 mm. ....	12
Figure 5. TEM images at a magnification of 60,000× for 10 weight-percent CTBN-modified DGEGBF, SC15, and SC79 resins.....	14
Figure 6. FESEM images of CTBN-modified DGEGBF, SC15, and SC79 with 0 and 10 weight-percent silica modification.....	15

---

## List of Tables

---

Table 1. SC-15 resin formulations. ....	2
Table 2. SC-79 resin formulations. ....	2
Table 3. SC-15 resin properties. ....	8
Table 4. SC-79 resin properties. ....	9
Table 5. End notch flexure (ENF) mode II properties. ....	11
Table 6. Drop tower impact properties. ....	11
Table 7. Summary of short beam shear and flexural strengths.....	12
Table 8. Tensile properties for 0 and 10 weight-percent silica-modified resin and composite. ....	13
Table 9. Fracture toughness comparisons between a model and VARTM epoxies. ....	14

---

## **Acknowledgments**

---

This research was also supported in part by an appointment to the research participation at the U.S. Army Research Laboratory (ARL) administered by the Oak Ridge Institute for Science and Education through an interagency agreement between the U.S. Department of Energy and ARL.

INTENTIONALLY LEFT BLANK.

---

## 1. Introduction

---

Vacuum-assisted resin transfer molding (VARTM) is a low-cost, efficient method for processing fiber-reinforced composites. Thermosetting resins utilizing VARTM techniques are required to have a viscosity lower than 1000 cP and long working times. Furthermore, resins that cure at room temperature are of particular interest due to reduction of residual stresses in the final part, energy costs for curing, and effects of thermal expansion mismatches between the composite constituents. A major drawback with VARTM resins is low fracture energies. Many techniques have been used to increase the fracture toughness of these polymer systems. One of the most common toughening methods involves adding soluble rubber modifiers that phase separately into micron-sized particles during cure (1, 2). Fracture energies have been increased by an order of magnitude for amine-cured epoxy resins modified with acrylonitrile-butadiene rubber modifiers (3). Another method for improving toughness has been the addition of inorganic inclusions. Lee and Yee reported three-fold increases in fracture toughness of an amine-cured epoxy with approximately 25- $\mu\text{m}$  glass particles (4).

Recent work by Kinloch et al. (5) and Sprenger et al. (6, 7) has shown a synergistic toughening effect by adding rubber and inorganic nanosilica to a diglycidyl ether of bisphenol-F (DGEBF) epoxy cured with diethyltoluene diamine. The addition of each individual modifier mildly increases toughness. When 9 weight-percent carboxyl-terminated acrylonitrile-butadiene (CTBN) rubber is added to the system, the fracture toughness (critical strain energy release rate,  $G_{IC}$ ) increases from 100 to 410  $\text{J/m}^2$ . The addition of 7.8 weight-percent of 20-nm epoxy-functional silica increases  $G_{IC}$  to 390  $\text{J/m}^2$ . When a combination of CTBN and silica are added, resin fracture toughness was reported as high as 2000  $\text{J/m}^2$ . In this work, we seek to institute a synergistic toughening effect for rubber-modified SC15 and SC79 (Applied Polymeric) VARTM resins through the addition of a commercially available DGEBF-based resin containing 40 weight-percent epoxy-functional silica (Nanopox F400). The effect of silica content on resin properties such as viscosity, glass transition temperature ( $T_g$ ), and fracture toughness are studied. Glass-reinforced composites infused with SC15 and SC79 resins containing 0 and 10 weight-percent silica are evaluated with respect to mode II fracture, impact, short beam shear, tensile, and flexural properties. Finally, investigations of resin morphology are investigated using scanning electron microscopy (SEM) and transmission electron microscopy (TEM) to elucidate differences in the VARTM resins and the model DGEBF systems.

---

## 2. Experimental

---

### 2.1 Materials and Resin Formulations

SC15 and SC79 are commercial VARTM resins developed by Applied Polymeric Inc. (Benicia, CA). They are rubber-modified, epoxy-based resins that have low viscosity. Nanopox F400 (Hanse Chemie, Geesthacht, Germany) is a commercial resin comprising 40 weight-percent silica and 60 weight-percent DGEBA (Epon 862). The silica particles have an average diameter of 20 nm and are chemically functionalized with epoxy groups. The epoxy equivalent weight (EEW) of the aforementioned materials is 173, 162, 171, and 295 g per equivalence for SC15, SC79, Epon 862, and Nanopox, respectively. The resin formulations studied in the work are given in tables 1 and 2. All systems were cured at 60 °C for 2 hr and 177 °C for 6 hr.

Table 1. SC-15 resin formulations.

Silica Content (weight-percent)	DGEBA Content (weight-percent)	EEW (g/equiv.)	Weight Fraction		
			SC-15 Part A	SC-15 Part B	Nanopox F 400
0	0	173.0	0.769	0.231	0.000
1	1.50	177.0	0.746	0.229	0.025
2.5	3.78	182.8	0.712	0.226	0.063
5	7.50	192.5	0.656	0.219	0.125
7.5	11.28	202.0	0.602	0.211	0.188
10	15.00	211.2	0.549	0.201	0.250
15	22.50	228.6	0.448	0.177	0.375

Table 2. SC-79 resin formulations.

Silica Content (weight-percent)	DGEBA Content (weight-percent)	EEW (g/equiv.)	Weight Fraction		
			SC-79 Part A	SC-79 Part B	Nanopox F 400
0	0	162.0	0.714	0.286	0.000
1	1.50	166.6	0.691	0.284	0.025
2.5	3.78	173.6	0.656	0.281	0.063
5	7.50	184.9	0.601	0.274	0.125
7.5	11.28	195.9	0.548	0.265	0.188
10	15.00	206.5	0.497	0.253	0.250
15	22.50	226.3	0.401	0.224	0.375

Additional materials were purchased to compare SC15 and SC79 to the model epoxy system developed by Kinloch et al. (5) and Sprenger et al. (6, 7). Epon 862 and diethyltoluene diamine (Epicure W) were purchased from Resolution Performance Products (Houston, TX). CTBN (Noveon, Cleveland, OH) was used as the model rubber modifier.

## 2.2 Resin Characterization

Three-point, single-edge notch bend (SENB) specimens were used for fracture toughness measurements. ASTM D 5045-93 (8) specifies that the sample dimensions of  $50 \times 12.5 \times 6.25 \text{ mm}^3$  to assure plain strain conditions. An initial crack was made by creating a notch in the specimens a distance that was half the sample thickness. A sharp razor blade was used to initiate a crack at the base of the notches. Approximately 10 samples were tested for each resin system. The samples were tested using an Instron 4505 equipped with a three-point bend fixture, a 1-kN load cell, and tested at a crosshead speed of 10 mm/min. All tests were performed at ambient conditions. When tests were completed, the fracture surfaces of all specimens were examined for signs of plastic deformation. If plastic deformation was apparent, the sample was not included in the reported results. The critical-stress-intensity factor ( $K_{IC}$ ) and critical strain energy release rate ( $G_{IC}$ ) at a span (S) to width (W) ratio of 4 are defined by the following expressions:

$$G_{IC} = \frac{(1-\nu^2)K_{IC}^2}{E}, \quad (1)$$

where

$$K_{IC} = (PBW^{1/2})f(x), \quad (2)$$

and

$$f(x) = 6x^{1/2} \frac{[1.99 - x(1-x)(2.15 - 3.93x + 2.7x^2)]}{(1+2x)(1-x)^{3/2}}, \quad (3)$$

and

$P$  = load,  
 $B$  = sample thickness,  
 $W$  = sample width,  
 $a$  = crack length,  
 $x = 0.45 < a/W < 0.55$ ,  
 $E$  = modulus, assumed 2.0 GPa for SC15 and SC79, and  
 $\nu$  = Poisson's ratio, assumed 0.35 for SC15 and SC79.

A TA Instruments dynamic mechanical analyzer (DMA), DMA Q800, with a 20-mm dual cantilever clamp frame was used to evaluate the storage modulus,  $E'$ , and  $T_g$  of each resin system. Temperature scans with an oscillation frequency of 1 Hz were performed at a rate of  $2 \text{ }^\circ\text{C}/\text{min}$  starting from  $-20$  to  $160 \text{ }^\circ\text{C}$  for SC15 and to  $230 \text{ }^\circ\text{C}$  for SC79. The  $T_g$  was taken as the peak of the loss modulus,  $E''$ , curve. Resin viscosity was measured using an AR2000 rheometer. All viscosities were reported at a constant shear rate of  $300 \text{ s}^{-1}$ .

### 2.3 Composite Characterization

S2 glass-reinforced composite panels with approximate dimensions of  $90 \times 60 \times 5 \text{ mm}^3$  were fabricated using the VARTM process (9). The woven fabric was stacked using  $0^\circ$ – $90^\circ$  fabric lay-ups. The S2 glass consisted of nominal 24 oz/yd<sup>2</sup> plain-woven  $5 \times 5$ , 250-yield roving with 463 sizing (the roving was made by Advanced Glassfiber Yarns and woven by Knytex – product SBA240F). SC15 and SC79 resins with 0 and 10 weight-percent silica were fabricated following the formulations and cure schedule outlined in section 2.1. Final volume fractions of glass fiber present in the composite panels were typically found to lie between 0.51 and 0.53 for all samples tested. Void content of the cured composite panels was not determined but was known to be consistently near 2% for this process (10).

Mode II composite properties were measured using an end notched flexure (ENF) specimen. Typical sample dimensions are given in figure 1. The initial crack length was formed by adding a 0.0005-in-thick Teflon\* spacer at the middle interlayer during composite fabrication. The crack length,  $a$ , was 50 mm, and  $L$  was chosen to be 100 mm so that the ratio of  $a/L$  was 0.5. Sample width,  $b$ , and thickness,  $h$ , were 20 and 2.5 mm, respectively. Samples were subjected to a three-point bend at a crosshead speed of 2.5 mm/min.

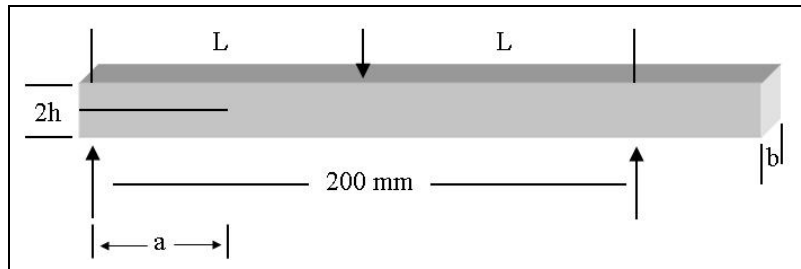


Figure 1. Sample geometry of ENF specimens.

The compliance method, given as  $\tau_{\max}$ , was used to determine the mode II strain energy release rate,  $G_{IIc}$ . In reality, the relationship between compliance,  $C$ , and crack length,  $a$ , was much more complicated for the ENF test than for mode I measurements. Although many equations have been proposed, the following equation accounting for modulus based on classic beam theory has been most widely used:

$$\tau_{\max} = \frac{3P_{\max}}{4bt}, \quad (4)$$

and

$$E' = \frac{2L^3 + 3a^3}{8Cbh^3}, \quad (5)$$

\*Teflon is a registered trademark of E.I. duPont de Nemours and Company.

where  $E'$  is the effective Young's modulus and  $L$  is the half-span length. Therefore, the expression for  $G_{IIc}$  is obtained for small values of  $(E'E/G_s)(h/a)^2$ , where  $G_s$  is the interlaminar shear modulus and is given by the following:

$$G_{IIc} = \frac{9a^2 P \delta}{2b(2L^3 + 3a^3)}. \quad (6)$$

Several criteria have been developed by the European Structural Integrity Society (ESIS) to establish crack initiation. Figure 2 shows a typical load-displacement curve for an ENF test. Crack initiation is defined as the point of deviation from initial slope linearity (NL), the point of intersection between a line with a 5% offset in initial slope and the load-displacement data (5% offset), or the maximum load value (Max).

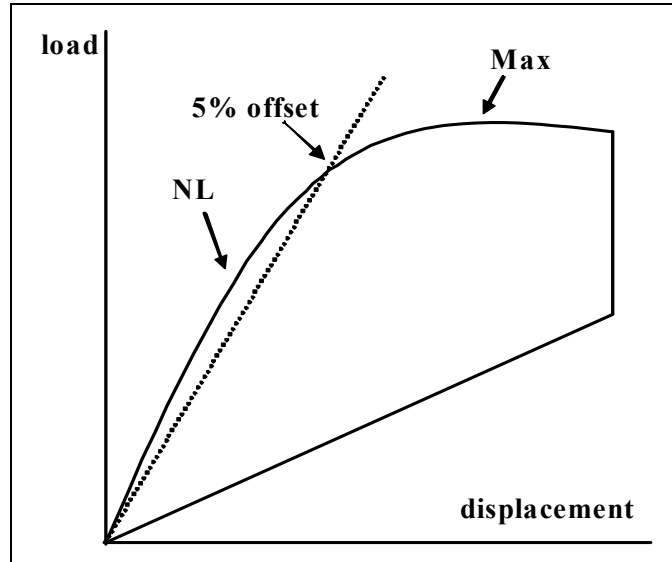


Figure 2. Alternative ESIS crack initiation criteria for ENF test methods (11).

The impact properties of the composite panels were measured using a Dynatup Drop Weight System. Samples were cut into  $100 \times 100 \times 5 \text{ mm}^3$  squares and impacted with a 12.7-mm diameter hemispherical impact striker. Experimentally measured values of impact energy ( $E_{\text{impact}}$ ), impact velocity ( $V_{\text{impact}}$ ), and maximum force ( $P_{\text{max}}$ ) were recorded from the instrument and are summarized in the results section. The impact energy absorbed to maximum force ( $E_{\text{max}}$ ) and total energy absorbed ( $E_{\text{total}}$ ) were calculated using the instrument software (12). Deflection data were not recorded. To measure the projected postimpact damage area, a digital image was taken of each damaged panel on a light box, and a pixel area ratio of the projected damaged area to the undamaged area was analyzed using an image analysis software package (13). Actual projected damage area could then be determined by multiplying the actual sample dimensions by

the computer-generated pixel ratio. Minimums of five samples were tested for each composite panel set.

The short-beam shear strength ( $S_H$ ) of each composite system was tested following ASTM D 2344-84 (14). Five specimens were tested for each composite. Each specimen was subjected to a three-point bend using an Instron model 4505 equipped with a 4.45-kN load cell and a crosshead rate of 1.27 mm/min. The span (s)-to-depth (d) ratio was approximately 4:1. The short-beam shear strength was calculated using the following equation, where  $P$  is the measured force at failure:

$$S_H = \frac{3P_B}{4bd}. \quad (7)$$

Flexural strength was measured with 80- × 12.5- × 5-mm composite panel samples using the ASTM D 790 (15) testing method. The test was carried out in the three-point bending mode configuration. Testing was completed with the span length (L)-to-width (b) ratio set to the standard 16:1 using a minimum of five samples for each composite formulation. An Instron model 4505 equipped with a 4.45-kN load cell was used at a cross-head rate of 1.27 mm/min. The equation used to calculate flexural modulus ( $E_{flex}$ ) is given next, where the slope of the tangent (m) is found by drawing a tangent to the steepest initial straight-line portion of the load-deflection curve. Breaking force ( $P$ ) was taken from force vs. displacement data, and the maximum fiber stress ( $\sigma_{max}$ ) was calculated using the following equations.

$$E_H = \frac{L^3 m}{4bd^3}, \quad (8)$$

and

$$\sigma_{max} = \frac{3PL}{2bd^2}, \quad (9)$$

where  $d$  is the depth of the specimen.

Tensile properties for the SC-15 and SC-79 epoxies and composites were evaluated according to ASTM D 3039 (16). An Instron 1125 universal testing frame was used to gather load data and failure stress values. A 5-kN load cell was used for the SC-79 and SC-15 epoxy specimens, and a 100-kN load cell was used for the composite systems. Strain data was obtained for the specimens utilizing a video image correlation (VIC) system. Testing was conducted in displacement control, with displacement rates adjusted so the engineering strain rate was 0.001/s for each specimen size (~6.0 mm/min). Two valid tests were conducted for each material and composite system.

The VIC system is a noncontact strain measurement method in which two cameras are used to capture video of the specimen during the deformation process. By first introducing a “speckle”

pattern of black and white dots on the gage portion of the specimen, it is possible to track the deformation of the sample by tracking the movement of the pattern on the surface. This is accomplished in real time by simultaneously recording load data during video capture. After calibrating the camera orientation and position using a customized grid of dots and fiduciary circles, it is possible to calculate the displacement and strain of the specimen. The VIC is beneficial over conventional strain measurement techniques because it measures displacement directly off the specimen gage length, unlike a linear voltage displacement transducer or typical strain gage that first convert global displacement into electrical signal. Additionally, once displacement data is correlated for a specimen, it is relatively facile to evaluate a more plenary set of mechanical properties for the material. These include, but are not limited to, elastic modulus, shear modulus, and Poisson's ratio. The VIC system used for the SC-15 and SC-79 epoxies and composites was a hardware and software package developed by Correlated Solutions Incorporated. Mono 12-bit Retiga OEM cameras fitted with Micro Nikkor 105-mm lenses were used for video capture. Video and load data were recorded using VicSnap software version 3.0D, and analysis was carried out on Vic-3D software version 2006 0.0. The ultimate tensile strength ( $F^{tu}$ ), Young's modulus ( $E$ ), and Poisson's ratio ( $\nu$ ) were calculated using the following equations:

$$F^{tu} = \frac{P}{bd}, \quad (10)$$

$$E = \frac{\Delta\sigma}{\Delta\varepsilon}, \quad (11)$$

and

$$\nu = \frac{\Delta\varepsilon_{lateral}}{\Delta\varepsilon_{longitudinal}}. \quad (12)$$

## 2.4 Morphological Characterization

The rubber morphology for the various epoxy systems was evaluated with a field emission scanning electron microscope (FESEM), Hitachi model S4700, using an acceleration voltage ranging between 3 and 5 kV. All samples were gold sputtered prior to SEM evaluation. The surfaces inspected with the FESEM were obtained from the fracture surface of the specimens used in the SENB experiments.

TEM was used to inspect the dispersion of silica in the epoxy matrices. A Leica Ultracut UCT microtome with a diamond knife was utilized to cut sections approximately 300 Å in thickness that were subsequently collected upon Formvar-coated TEM grids. TEM was completed using JEOL 200 CX instrument operated at a 120-kV accelerating voltage.

---

### 3. Results and Discussion

---

The purpose of this work was to translate a synergistic toughening effect between nanosilica and rubber modifiers from a model DGEGBF system studied in literature (5–7) to commercial, elastomer-modified VARTM epoxy resin systems (SC15 and SC79). First, resin properties, such as fracture toughness, T<sub>g</sub>, and viscosity, were evaluated with varying levels of silica content. Second, the most promising resin formulations were manufactured in glass-reinforced composites. The composite properties evaluated included mode II fracture toughness, impact, short beam shear (SBS), flexural, and tensile properties. Finally, TEM and FESEM techniques were used to compare the rubber and silica morphology of the model epoxy system to the VARTM resins. This analysis allowed for the formulation of hypotheses explaining the resin and composite properties.

#### 3.1 Resin Properties

The rationale of silica addition is to improve fracture toughness of the rubber-modified VARTM resins without sacrificing other resin properties such as viscosity, T<sub>g</sub>, and modulus. A summary of SC15 and SC79 properties with varying silica concentrations is given in tables 3 and 4, respectively. Figure 3 gives a plot of the fracture toughness as silica concentration increases. Since silica is premixed with a DGEGBF monomer, increasing silica content also increases the amount of DGEGBF in the system. In addition to the effects of silica on resin properties, DGEGBF will also influence resin properties by changing the overall EEW of the epoxy monomers. To distinguish the effects of silica addition from DGEGBF, the fracture toughness of DGEGBF cured with stoichiometric amounts of respective curing agents was found. The fracture toughness of DGEGBF cured with SC15 and SC79 amines was  $700 \pm 60 \text{ J/m}^2$  and  $260 \pm 30 \text{ J/m}^2$ , respectively. By using a rule-of-mixtures approach, the fracture toughness of SC epoxies and DGEGBF could be predicted. These predictions are represented as dashed lines in figure 3. Any deviations from the dashed line can be assumed as the influence of the silica.

Table 3. SC-15 resin properties.

Silica Content (weight-percent)	Viscosity (cP)	T <sub>g</sub> (°C)	E' at 25 °C (GPa)	K <sub>Ic</sub> (MPa·m <sup>0.5</sup> )	G <sub>Ic</sub> (J/m <sup>2</sup> )
0	280	94.1	2.37	1.70 ± 0.16	900 ± 170
1	440	94.7	2.44	1.89 ± 0.11	1020 ± 110
2.5	480	98.1	2.31	1.86 ± 0.21	720 ± 100
5	460	99.8	2.49	1.67 ± 0.12	790 ± 140
7.5	520	99.4	2.61	1.77 ± 0.16	790 ± 120
10	580	97.3	2.37	1.73 ± 0.10	880 ± 70
15	1130	93.1	2.96	1.74 ± 0.09	700 ± 100

Table 4. SC-79 resin properties.

Silica Content (weight-percent)	Viscosity (cP)	T <sub>g</sub> (°C)	E' at 25 °C (GPa)	K <sub>1c</sub> (MPa·m <sup>0.5</sup> )	G <sub>1c</sub> (J/m <sup>2</sup> )
0	220	180.0	2.91	1.04 ± 0.29	180 ± 60
1	250	179.4	2.84	0.70 ± 0.13	90 ± 40
2.5	300	174.4	2.66	1.03 ± 0.41	240 ± 130
5	370	174.0	2.83	0.93 ± 0.21	230 ± 100
7.5	430	167.7	3.01	1.03 ± 0.39	200 ± 90
10	490	165.3	3.35	1.06 ± 0.18	380 ± 50
15	1090	162.3	2.91	1.27 ± 0.08	250 ± 60

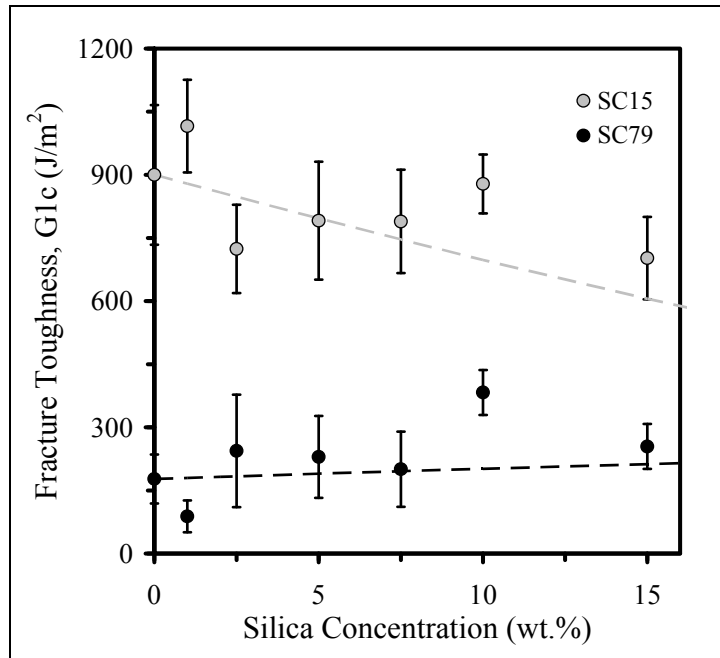


Figure 3. A plot of fracture toughness ( $G_{1c}$ ) as a function of silica concentration in SC15 and SC79 resins. A rules-of-mixture line is shown for each resin that accounts for the change in fracture toughness as a result of blending DGEBF into the formulation.

According to figure 3, the influence of DGEBF is more prominent than the presence of silica. For SC15, the DGEBF had a lower EEW than the epoxy part of the SC15. Therefore, the overall crosslink density of the matrix phase increased and caused the resin to become more brittle. Increasing silica content and thus the concentration of DGEBF inherently reduced the fracture toughness of the system. A most promising silica-modified formulation occurred at 10 weight-percent silica. The  $G_{1c}$  of this formulation,  $880 \pm 70 \text{ J/m}^2$ , was essentially equal to the baseline resin ( $900 \pm 170 \text{ J/m}^2$ ). Composite properties using this formulation will be addressed in the subsequent section.

The addition of Nanopox has the opposite effect on SC79. Since DGEGBF had a higher EEW than the SC79 epoxy, the overall EEW of the system increased and matrix crosslink density decreased. At most silica concentrations shown in figure 3, the influence of silica appears to be minor. At 10 weight-percent silica, however, the combination of decreased crosslink density and the presence of silica yielded the highest fracture toughness. The  $G_{IC}$  was improved from  $180 \pm 60 \text{ J/m}^2$  for the unmodified SC79 to  $380 \pm 50 \text{ J/m}^2$ . This resin formulation will be used to evaluate composite properties in the next section.

In addition to fracture toughness, resin properties such as viscosity and  $T_g$  are affected by Nanopox modification. The DGEGBF contained in Nanopox has a higher viscosity than the SC15 and SC79 epoxy parts. Therefore, as increasing silica content increases, the viscosity will increase due to the coupled DGEGBF. Increased viscosity does not become a factor in VARTM processing until the viscosity is above 1000 cP. As shown in tables 3 and 4, all formulations with silica content of 10 weight-percent and lower would not create processing issues. However, 15 weight-percent silica yielded viscosities over 1000 cP and cannot be utilized as VARTM resins.

The fracture toughness results indicated a strong influence of DGEGBF on the crosslink density. The matrix crosslink density also impacted the  $T_g$  in thermosetting polymers. For SC15, the  $T_g$  was not strongly affected by the addition of Nanopox. The largest improvement in  $T_g$  occurred at 5 weight-percent silica, increasing from 94.1 to 99.8 °C. Further, Nanopox modification slightly decreased the  $T_g$ . The SC79 system showed a stronger influence of DGEGBF on  $T_g$ . This property steadily decreased from 180 to 162.3 °C (15 weight-percent silica).

### 3.2 Composite Properties

The previous section demonstrated that 10 weight-percent silica had the highest toughness performance for both resin systems. Therefore, composites were made comprising 10 weight-percent silica and were compared to both baseline resin systems. ENF is an effective technique for comparing mode II fracture toughness in fiber-reinforced composites. Table 5 summarizes all of the results from the ENF tests. As was discussed in the experimental section, there are three points that can be used to define the point of crack propagation. These criteria (nonlinearity, 5% offset of initial slope, and maximum load) are presented. The trends are the same for each criterion, so we will focus on the 5% offset data in our discussion. For SC15, the addition of 10 weight-percent silica reduced  $G_{II}$  from  $1240 \pm 80 \text{ J/m}^2$  to  $990 \pm 90 \text{ J/m}^2$ . The SC79 system showed the opposite trend, where silica addition improved  $G_{II}$  from  $590 \pm 20 \text{ J/m}^2$  to  $720 \pm 70 \text{ J/m}^2$ . These results reinforced the trends shown in the resin systems. The combination of decreased matrix crosslink density and the addition of silica improved SC79 resin and composite toughness. The increased crosslink density in SC15 detracted from any potential improvements provided by the silica.

Table 5. End notch flexure (ENF) mode II properties.

Resin	Silica Content (weight-percent)	Nonlinearity $G_{II}$ ( $J/m^2$ )	5% Offset $G_{II}$ ( $J/m^2$ )	Maximum Load $G_{II}$ ( $J/m^2$ )
SC-15	0	370 ± 40	1240 ± 80	3130 ± 370
	10	300 ± 30	990 ± 90	2840 ± 170
SC-79	0	150 ± 30	590 ± 20	1580 ± 80
	10	210 ± 40	720 ± 70	2100 ± 400

Drop tower experiments were carried out to correlate the resin and composite toughness to ultimate impact properties. Table 6 gives the tabulated results of these experiments. Each composite was impacted with approximately 103 J of energy. The total energy absorbed by the composite,  $E_{total}$ , correlated to the amount of impact energy absorbed by the composite. Therefore, a tough composite would have a relatively low  $E_{total}$ , high impact load ( $P_{max}$ ), high energy absorbed at maximum load ( $E_{max}$ ), and a minimal damage area. SC15 showed negligible difference in impact load and total energy absorbed. The most significant difference was the size of the damage area. The addition of Nanopox increased the damage area from  $950 \pm 80 \text{ mm}^2$  to  $1340 \pm 130 \text{ mm}^2$ , thus indicating a reduction in overall composite toughness and impact properties. Figure 4 shows the strike face of damaged panels for the SC15 and SC79 systems.

Table 6. Drop tower impact properties.

Resin	Silica Content (weight-percent)	$E_{impact}$ (J)	$P_{max}$ (kN)	$E_{max}$ (J)	$E_{total}$ (J)	Damage Area ( $\text{mm}^2$ )
SC15	0	103.0 ± 0.8	16.2 ± 0.2	88.5 ± 4.0	79.7 ± 2.2	950 ± 80
	10	103.3 ± 0.3	15.7 ± 0.5	87.7 ± 10.1	79.3 ± 5.4	1340 ± 130
SC79	0	103.1 ± 0.3	15.7 ± 0.5	66.6 ± 2.2	89.6 ± 2.6	2280 ± 210
	10	102.7 ± 0.2	15.4 ± 0.5	67.3 ± 6.0	84.3 ± 2.0	2040 ± 150

The impact properties of the SC79 systems were more sensitive to silica addition than the SC15 resins. Although there was no difference in impact load, there were substantial differences in total energy absorbed and damage area. When silica was present in the resin,  $E_{total}$  decreased from  $89.6 \pm 2.6 \text{ J}$  to  $84.3 \pm 2.0 \text{ J}$  and damage area reduced from  $2280 \pm 210 \text{ mm}^2$  to  $2040 \pm 150 \text{ mm}^2$ . The improvement in resin and composite toughness by adding Nanopox translated directly to impact properties.

In addition to toughness and impact properties, structural properties (SBS, flexural, and tensile strengths) were also investigated, summarized in table 7. SBS properties were generally influenced by the interfacial performance of the fiber with the polymer matrix. The addition of silica had very little effect on these properties. SC15 showed a slight reduction from  $47.8 \pm 0.9 \text{ MPa}$  to  $44.4 \pm 1.6 \text{ MPa}$ . For SC79, a minor increase from  $34.7 \pm 5.4 \text{ MPa}$  to  $35.8 \pm 1.1 \text{ MPa}$  occurred.

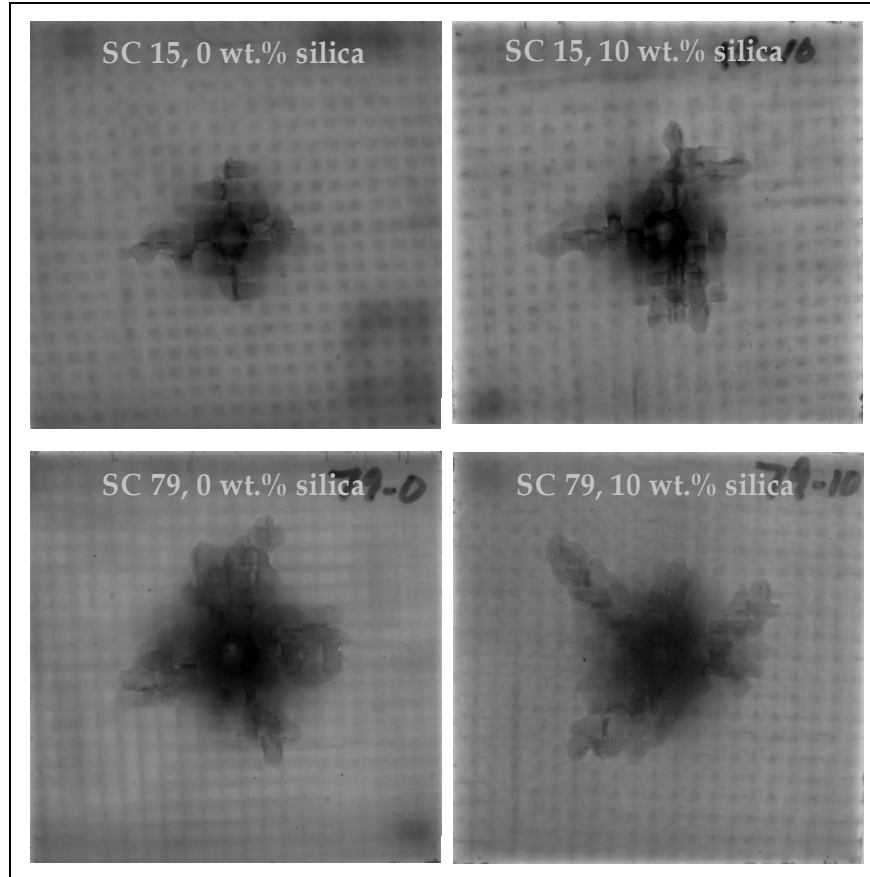


Figure 4. Digital images of the composite strike face after drop tower impact testing. Imaging software is used to calculate the damage area. Each panel image is 100 × 100 mm.

Table 7. Summary of short beam shear and flexural strengths.

Resin	Silica Content (weight-percent)	SBS	Flexural Tests	
		$S_H$ (MPa)	$\sigma_{max}$ (MPa)	$E_H$ (GPa)
SC15	0	47.8 ± 0.9	404.3 ± 41.8	22.1 ± 0.9
	10	44.4 ± 1.6	464.1 ± 24.2	24.4 ± 0.8
SC79	0	34.7 ± 5.4	441.0 ± 30.0	24.9 ± 1.6
	10	35.8 ± 1.1	366.2 ± 13.8	25.1 ± 0.9

Table 7 indicates that the maximum fiber stress,  $\sigma_{max}$ , is more sensitive to silica modification than modulus of elasticity,  $E_H$ , with respect to flexural experiments. Upon silica addition,  $E_H$  slightly changed from 22.1 ± 0.9 MPa to 24.4 ± 0.8 MPa for SC15 and from 24.9 ± 1.6 MPa to 25.1 ± 0.9 MPa for SC79. For  $\sigma_{max}$ , SC15 substantially increased from 404.3 ± 41.8 MPa to 464.1 ± 24.2 MPa, while a decrease from 441.0 ± 30.0 MPa to 366.2 ± 13.8 MPa was found for SC79. Again, these trends were more indicative of a change in crosslink density than to any silica addition.

Resin and composite tensile properties, given in table 8, were measured for the SC15 and SC79 systems. In general, a toughened resin or composite resulted in decreased structural properties. For SC15, resin and composite toughness decreased with the addition of silica, accompanied with an increase in tensile properties. These trends were more evident in the resin, where Young's modulus (E) and ultimate tensile strength ( $F^{tu}$ ) increased from 2.63 to 3.46 GPa and 30.5 to 38.3 MPa, with the addition of 10 weight-percent silica, respectively. Although the composite structural properties were influenced more by the glass reinforcement than the resin, the SC15 composite data showed similar trends to the resin data. The E and  $F^{tu}$  increased from 18.17 to 18.76 GPa and 320.6 to 487.9 MPa, with 10 weight-percent silica addition. As was also seen in the toughness data, adding silica had the opposite effect on SC79. The resin E and  $F^{tu}$  decreased from 4.10 to 3.25 GPa and 27.7 to 16.5 MPa, respectively. The composite E and  $F^{tu}$  decreased from 22.13 to 22.01 GPa and 419.5 to 380.1 MPa, respectively.

Table 8. Tensile properties for 0 and 10 weight-percent silica-modified resin and composite.

Resin	Silica Content (weight-percent)	Resin			Composite		
		$F^{tu}$ (MPa)	E (GPa)	$\nu$	$F^{tu}$ (MPa)	E (GPa)	$\nu$
SC15	0	30.5	2.63	0.38	320.6	18.17	NA
	10	38.3	3.46	0.38	487.9	18.76	NA
SC79	0	27.7	4.10	0.41	419.5	22.13	0.19
	10	16.5	3.25	0.39	380.1	22.01	0.22

Note: NA = not available.

In general, resin properties directly translated to composite properties. The influence of DGEGBF on the crosslink density of the matrix exceeded any toughening effects associated with silica. Since DGEGBF had a lower EEW than the SC15 epoxy monomers, the matrix had a lower EEW and higher crosslink density. This corresponded to reduced fracture energies and impact properties. Adding DGEGBF to the SC79 resin system decreased the matrix crosslink density. This, combined with the presence of silica, resulted in mild improvements in toughness and impact properties. In addition to changing crosslink density, adding Nanopox reduced the overall rubber content. This may be another explanation for a lack of synergistic toughening in the VARTM resins. Finally, the presence of DGEGBF and nanosilica may potentially influence the phase separation of the rubber during cure. The next section will address any morphological changes.

### 3.3 Comparisons Between Model and VARTM Epoxies

According to resin and composite properties, synergistic toughening between an elastomer and nanosilica in epoxy did not translate from model epoxy systems to the VARTM epoxy resins. This section will identify differences between these systems that could be potential explanations for this behavior. The model epoxy system contained the same DGEGBF found in Nanopox (Epon 862). Therefore, adding a rubber modifier, CTBN, ensured that the concentration of all

components in these systems was known. SC15 and SC79 are proprietary resins in which the type and concentration of elastomer are unknown. Table 9 compares the fracture toughness ( $G_{IC}$ ) of a model 10 weight-percent CTBN-modified DGEBF system to the VARTM resins. This comparison further illustrated that the VARTM resins did not achieve a synergy between the rubber and silica. The model DGEBF resin was improved almost five-fold from the best VARTM resin (SC79, 10 weight-percent silica), whereas the best VARTM resin improvement was 111.1% for SC79.

Table 9. Fracture toughness comparisons between a model and VARTM epoxies.

$G_{IC}$ [=] $J/m^2$	10 Weight-Percent CTBN-Modified DGEBF	SC15	SC79
0 weight-percent silica	$390 \pm 70$	$900 \pm 170$	$180 \pm 60$
10 weight-percent silica	$1890 \pm 190$	$880 \pm 70$	$380 \pm 50$
Difference	+474.9%	-2.2%	+111.1%

One theory for a potential toughening mechanism in these systems is the phase in which the silica assembles. Figure 5 gives TEM images that are used to distinguish the rubber and silica in these systems. Comparing these systems, it was clear that the silica migrated into the epoxy phase during rubber phase separation. Therefore, silica assembly had a negligible influence with respect to the toughening effect in these systems. Future work will focus on ways of controlling silica migration to further disprove its importance as a toughening mechanism.

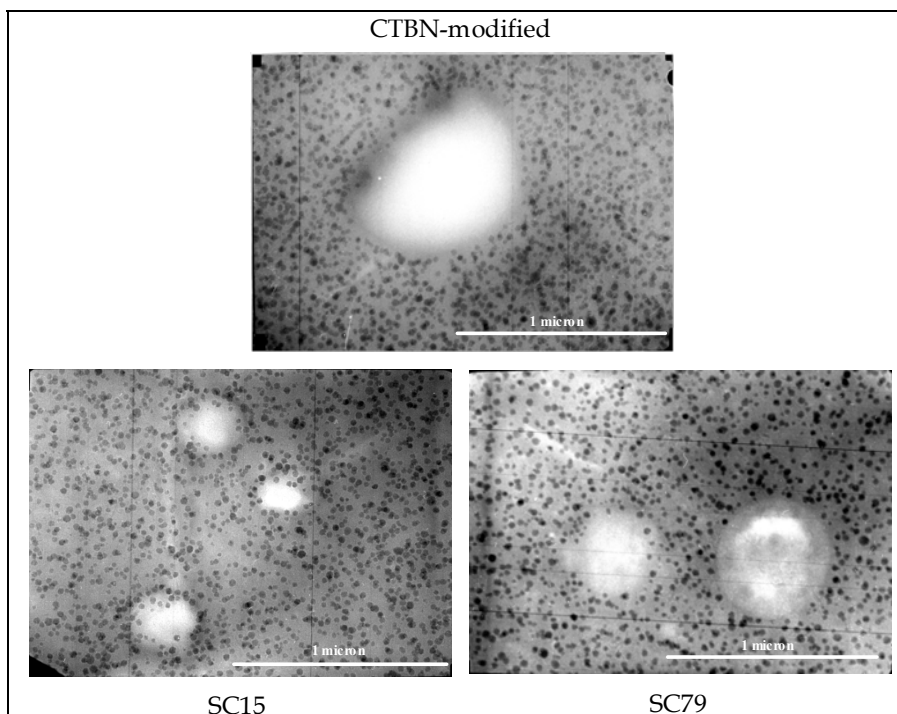


Figure 5. TEM images at a magnification of  $60,000\times$  for 10 weight-percent CTBN-modified DGEBF, SC15, and SC79 resins.

FESEM images were taken to compare the difference in rubber morphology for the various resin systems, given in figure 6. One noticeable observation for the CTBN-modified DGEBF system was the size and dispersion of the phase-separated rubber particles. The system without silica had larger particles more sparsely dispersed throughout the matrix. When 10 weight-percent silica was added to the system, the number of particles increased, the particle size decreased, and the particles were more closely dispersed. A likely explanation was that the silica forced more nucleation sites for the rubber particles. The dispersion of the rubber could be a potential factor in toughening. Future work will focus on studying factors about the model DGEBF system that make it suitable for synergy between rubber and silica modifiers. We will investigate methods of controlling rubber phase morphology to determine whether the way in which silica influences phase separation is the predominant toughening mechanism.

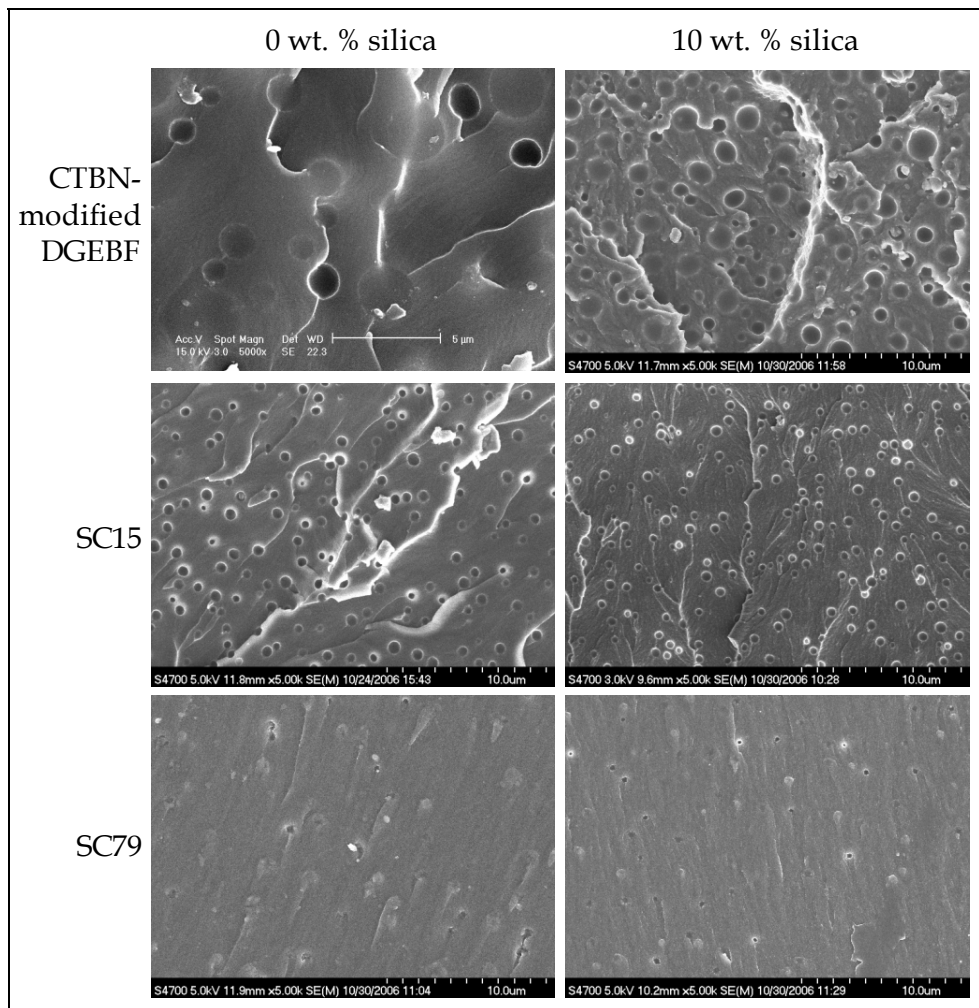


Figure 6. FESEM images of CTBN-modified DGEBF, SC15, and SC79 with 0 and 10 weight-percent silica modification.

---

## 4. Conclusion

---

The goal of this work was to achieve an enhanced fracture toughness of commercial VARTM epoxy resins (SC15 and SC79) through a synergy between nanosilica particles and elastomer modifiers. Nanopox is a commercial DGEGBF resin containing 40 weight-percent nanosilica particles. By blending the VARTM resins with various amounts of Nanopox, we were able to investigate the effect of silica concentration on resin properties, such as fracture toughness, viscosity, and  $T_g$ . The presence of DGEGBF in the Nanopox impacted matrix crosslink density, increasing for SC15 and decreasing for SC79. It was found that changing crosslink density was as influential in toughening as adding silica. Generally, SC15 experienced decreased toughening effects while SC79 showed slight increases in fracture toughness. Furthermore, SC79 containing 10 weight-percent silica increased fracture toughness from  $180 \pm 60 \text{ J/m}^2$  to  $380 \pm 50 \text{ J/m}^2$  and proved to be the most promising formulation. Glass-reinforced composite properties followed the same trends found for the resin properties. The SC15 composite showed that silica modification reduced mode II fracture toughness and impact properties due to decreased resin toughness. On the other hand, SC79 had improved mode II fracture toughness and impact properties. TEM and FESEM analysis showed that silica changed the dispersion and size of the rubber morphology in these systems. For a model DGEGBF system, rubber morphology was more significantly affected by silica than for the VARTM epoxies. Future work will further elucidate the effect of silica on rubber phase separation and potentially explain the reason that VARTM resins did not achieve a toughening synergy.

---

## 5. References

---

1. Collyer, A., Ed. *Rubber Toughened Engineering Plastics*; Chapman and Hall: London, 1994.
2. Riew, C., Ed. *Rubber Toughened Plastics*; American Chemical Society: Washington, 1989.
3. Pearson, R. A.; Yee, A. F. Toughening Mechanisms in Elastomer-Modified Epoxies. *J. Mater. Sci.* **1989**, *24*, 2571–2580.
4. Lee, J.; Yee, A. F. Role of Inherent Matrix Toughness on Fracture of Glass Bead Filled Epoxies. *Polymer* **2000**, *41*, 8375–8385.
5. Kinloch, A. J.; Lee, J. H.; Taylor, A. C.; Sprenger, S.; Eger, C. Toughening Structural Adhesives via Nano- and Micro-Phase Inclusions. *J. of Adhesion* **2003**, *79*, 867–873.
6. Sprenger, S.; Kinloch, A. J.; Taylor, A. C.; Mohammed, R. D.; Eger, C. Rubber-Toughened FRCs Optimized by Nanoparticles. *JEC Composites* **2005**, *9*, 73–76.
7. Sprenger, S.; Kinloch, A. J.; Taylor, A. C.; Mohammed, R. D.; Eger, C. Rubber-Toughened GFRCs Optimized by Nanoparticles. *JEC Composites* **2005**, *12*, 66–69.
8. ASTM D 5045-93. Standard Test Methods for Plane-Strain Fracture Toughness and Strain Energy Release Rate of Plastic Materials. Designation D 5045-99; American Society for Testing and Materials **1999**.
9. Hsiao, K. T.; Gillespie, J. W.; Advani, S. G.; Fink, B. K. Role of Vacuum Pressure and Port Locations on Flow Front Control for Liquid Composite Molding Processes. *Polymer Composites* **2001**, *22*, 660.
10. Ghiorse, S. R. U.S. Army Research Laboratory, Aberdeen Proving Ground, MD. Private communication, 15 August 2005.
11. De Morais, A. B.; Silva, J. F.; Marques, A. T.; De Castro, P. T. Mode II Interlaminar Fracture of Filament Wound Angle-Ply Specimens. *Appl. Comp. Mater.* **2002**, *9*, 117–129.
12. Instron Dynatup 930-1 (version 1.21) software.
13. Rasband, W. Image J (version 1.30). National Institutes of Health, Bethesda, MD, 2003.
14. ASTM D 2344-84. Standard Test Methods for Apparent Interlaminar Shear Strength of Parallel Fiber Composites by Short-Beam Method. Designation D 2344-84; American Society for Testing and Materials **1995**.

15. ASTM D 790. Standard Test Methods for Flexural Properties of Unreinforced and Reinforced Plastics and Electrical Insulating Materials. Designation D 790-96a; American Society for Testing and Materials **2003**.
16. ASTM D 3039. Standard Test Methods for Tensile Properties of Polymer Matrix Composite Materials. Designation D 3039/D 3039M-95a; American Society for Testing and Materials **2006**.

NO. OF  
COPIES ORGANIZATION

1 DEFENSE TECHNICAL  
(PDF INFORMATION CTR  
ONLY) DTIC OCA  
8725 JOHN J KINGMAN RD  
STE 0944  
FORT BELVOIR VA 22060-6218

1 US ARMY RSRCH DEV &  
ENGRG CMD  
SYSTEMS OF SYSTEMS  
INTEGRATION  
AMSRD SS T  
6000 6TH ST STE 100  
FORT BELVOIR VA 22060-5608

1 DIRECTOR  
US ARMY RESEARCH LAB  
IMNE ALC IMS  
2800 POWDER MILL RD  
ADELPHI MD 20783-1197

3 DIRECTOR  
US ARMY RESEARCH LAB  
AMSRD ARL CI OK TL  
2800 POWDER MILL RD  
ADELPHI MD 20783-1197

ABERDEEN PROVING GROUND

1 DIR USARL  
AMSRD ARL CI OK TP (BLDG 4600)

INTENTIONALLY LEFT BLANK.